(1992); D. R. Blake *et al., ibid.* **99**, 1699 (1994); D. R. Blake *et al., ibid*., in press.
7. M. E. Ruiz S., K. Gerner, M. Y. Barbiaux S., R. Seila, paper presented at the 86th Annual Meeting of the Air and Waste Management Association, Denver, CO, 13 to 18 June 1993.
8. In (*2*), vol. 3, p. 94.
9. A list of 67 identified options for improving air quality in Mexico City is given in (*2*), vol. 5, pp. 7–8.
10. B. J. Finlayson-Pitts, and J. N. Pitts Jr., *Air Waste* **43**, 1091 (1993); *Atmospheric Chemistry: Fundamentals and Experimental Techniques* (Wiley, New York, 1986).
11. National Research Council, *Rethinking the Ozone Problem in Urban and Regional Air Pollution* (National Academy Press, Washington, DC, 1991).
12. In (*11*), pp. 231–237.
13. R. Atkinson, *J. Phys. Chem. Ref. Data*, Monograph 1 (1989); R. Atkinson *et al., ibid.* **18**, 881 (1989).
14. W. P. L. Carter, *Air Waste* **44**, 881 (1994).
15. In (*2*), vol. 3, pp. 34–35.
16. W. L. Chameides *et al., J. Geophys. Res.* **97**, 6037 (1992); in (*11*), p. 234.
17. J. H. Seinfeld, *Science* **243**, 745 (1989).
18. In (*2*), vol. 4, pp. 73–74.
19. In (*11*), pp. 354–356.
20. In (*2*), vol. 2, p. 22.
21. In (*2*), vol. 3, p. 88.
22. R. L. Seila and W. A. Lonneman, paper 88-150,8, presented at the 81st Annual Meeting of Air Pollution Control Association, Dallas, Texas, 20 to 24 June 1988; quoted in (*17*).
23. H. Singh and P. Zimmerman in *Gaseous Pollutants: Characterization and Cycling*, J. O. Nriagu, Ed. (Wiley, New York, 1992), pp. 177–235; N. J. Blake, D. R. Blake, T.-Y. Chen, T. W. Smith Jr., F. S. Rowland, paper presented at the American Geophysical Union Meeting, San Francisco, CA, December 1993.
24. Supported by the Department of Energy through Contract W-GEC 91-122 with the western branch (WESTGEC) of the National Institute of Global Environmental Change (NIGEC). The analytical equipment for the four- and six-aliquot gas chromatographic determinations was purchased with a grant from the Keck Foundation.

28 April 1995; accepted 20 July 1995

Polar Standstill of the Mid-Cretaceous Pacific Plate and Its Geodynamic Implications

John A. Tarduno and William W. Sager

Paleomagnetic data from the Mid-Cretaceous Mountains suggest that Pacific plate motion during the Early to mid-Cretaceous was slow, less than 0.3 degree per year, resembling the polar standstill observed in coeval rocks of Eurasia and North America. There is little evidence for a change in plate motion that could have precipitated the major volcanic episode of the early Aptian that is marked by the formation of the Ontong Java Plateau. During the volcanism, oceanic plates bordering the Pacific plate moved rapidly. Large-scale northward motion of the Pacific plate began after volcanism ceased. This pattern suggests that mantle plume volcanism exerted control on plate tectonics in the Cretaceous Pacific basin.

An extraordinary episode of volcanism that was marked by the creation of several large oceanic plateaus affected the Pacific Ocean basin during the Cretaceous (*1–4*). In some models, the plateaus represent sites where mantle plumes first impinged on the oceanic lithosphere (*5*). The bulk of volcanism is represented in the Earth's largest oceanic plateau, the Ontong Java Plateau (OJP), which formed in the early Aptian (*3*). The relation between this large-scale volcanism and the tectonic development of the Pacific basin is unclear. Anderson (*6*), for example, suggested that changes in Pacific basin plate motion drove Cretaceous volcanism, negating the need for a deep mantle plume source. To examine the relation between early Aptian volcanism and plate tectonics, we examined the absolute motion of the Pacific plate from recent paleomagnetic data available through deep sea drilling in the Mid-Pacific Mountains (MPM) [Ocean Drilling Program (ODP) sites 865 and 866] (*7*) (Fig. 1). At site 866, an altered basaltic basement sequence was recovered beneath a thick (1622 m) sequence of shallow water limestone. Down the section, the basalts grade from submarine pillows to subaerial flows separated by weathered horizons (boles) (Fig. 2). Strontium and carbon isotopic (*8*) and paleontologic dating (*9*) of the basal sediments suggest that the basalts are of at least Hauterivian age [127 to 132 million years ago (Ma)] (*10*). $^{40}Ar/^{39}Ar$ radiometric age dating yields two age groups (123 Ma and 127.8 Ma) (*11*) that are broadly consistent with the other age estimates.

These data suggest that a paleolatitude estimate for the Pacific plate during the period before plateau-building volcanism might be available from the site 866 basalts. If the magnetization of the boles was acquired during weathering, they might provide an internal average of paleosecular variation (PSV). To test this hypothesis, three boles were sampled, in addition to the least altered basalts, for paleomagnetic analysis (*12*).

A large percentage of magnetization was lost between 550° and 580°C, which is characteristic of a magnetite carrier and a chemical remanent magnetization (*13*) (Fig. 3). In addition, most samples displayed a small remanence with unblocking temperatures >580°C, which is characteristic of hematite. In the basalt samples in which a clear hematite component was isolated (~30%), it was colinear with the magnetite magnetization. The sequence was of reversed polarity (positive inclination, Southern Hemisphere), with a reversed-to-normal polarity transition near the base of the hole. Thermal demagnetization of bole samples displayed similar unblocking characteristics but with a larger hematite contribution (Fig. 3).

If undetected, large-volume short-duration volcanism can bias the time-averaged field value derived from any lava sequence (*14*). A plot of inclination versus the basalt stratigraphy reveals several important clues to the origin of the magnetizations (Fig. 2). Although directions from bole B-2 are scattered, the three boles do not appear to

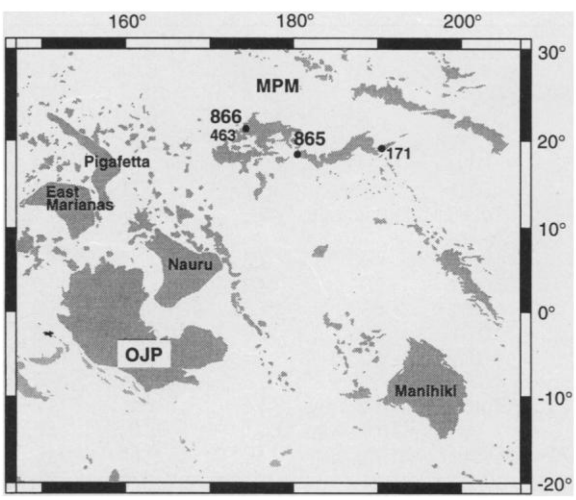

Fig. 1. Early Cretaceous (Aptian) volcanism represented on Manihiki Plateau and in the Nauru, Pigeffeta, and East Marianas basins has been linked to a mantle plume that formed the OJP (*3*). Alternatively, this volcanism is thought to result from a change in plate motions (*6*). Also shown are the MPM and the Deep Sea Drilling Project (DSDP) and ODP drill sites.

J. A. Tarduno, Department of Earth and Environmental Sciences, University of Rochester, Rochester, NY 14627, USA.
W. W. Sager, Department of Oceanography, Texas A&M University, College Station, TX 77843, USA.

average PSV because they do not record the same inclination value (*15*) (B-1 = 34.0° ± 2.9°, B-2 = 26.0° $^{+21.0°}_{-21.7°}$, and B-3 = 22.4° ± 9.2°). Instead their inclinations agree better with those of the immediately overlying flows (32.5° $^{+2.6°}_{-2.7°}$, 22.7°, and 20.2° ± 2.8°, respectively), which suggests local remagnetizations of the boles at the beginning of the next eruptive phase. This pattern implies that the basalt magnetizations retained the field value during cooling. We divided the data into inclination groups based on the observed boles, petrologic units, magnetic polarity, and lastly, distinct inclination values (*16*) (Fig. 2). On the basis of 13 inclination groups, we computed a mean paleolatitude (λ) for the site of 14.2° $^{+3.2°}_{-3.3°}$ S. There is no correlation between the inclination units and the two radiometric age dates; both dates are from reversed-polarity basalts. If the younger radiometric age dates are from sills, then the mean paleolatitude represents an average over several million years. Because there is no lithologic evidence in the sequence for sills (*7*), the younger ages may instead reflect alteration.

Limestone of reversed polarity chron M7r (*17*) overlies the basalts. Because the uppermost basalts are submarine, we believe there is no significant temporal break at the basalt-sediment interface. The reversed-to-normal field reversal near the base of the basalt section is assigned to the base of the reversed-polarity chron M7r (M7r → M8n), which lasted 0.36 million years (*10*). Approximately one-third of M7r may be represented by the lowest sediments (*17*); in this case the recovered basalt sequence would span over 200,000 years, which is sufficient to average PSV.

PSV can also be evaluated by examination of the directional angular dispersion (s), which is related to the best estimate of the precision of paleomagnetic directions (k) by

$$s^2 = 6561/k \tag{1}$$

We use the best estimate of the precision parameter (k) available from our inclination-only average (*15*). For comparison with available datasets, this directional dispersion must be expressed in terms of pole dispersion (*18*) (S):

$$S^2 = s^2 H[\lambda, s^2(\lambda)] \tag{2}$$

where the transformation function $H[\lambda, s^2(\lambda)]$ is obtained from Cox (*19*). The resulting estimate (S = 10°) is within the range (7° to 11°) quoted for the Early Cretaceous (*20*), which provides supporting evidence that PSV has been averaged.

Our data constrain the Early Cretaceous Pacific pole to fall on a small circle around the site with radius equal to the colatitude ($p = 90° - \lambda$). When compared with an apparent polar wander path (APWP) based on basalt colatitudes from other sites and the magnetic inversions of seamount magnetic anomalies (*21*), our data yield little evidence for latitudinal motion of the Pacific plate from the Early to mid-Cretaceous (Fig. 4). Comparison of our estimate with results from sediments is complicated because of compaction-induced shallowing of sediment inclination values (*22*). Only three sites (sites 463, 865, and 866) may have yielded data unaffected by compaction (*23, 24*). Together these sediment data sets also suggest that Pacific plate latitudinal motions were minor in the Early to mid-Cretaceous (Fig. 5). Because the basal sediments from site 866 indicate the same paleolatitude range as calculated from the basalts, the potential presence of sills in the section has little effect on these conclusions. A small southward drift is allowable between Aptian and Albian times postdating formation of OJP (*3*), as suggested by the data from site 463 (*24*).

The MPM are often reconstructed to the "superswell" of the modern south Pacific (*25*), an area characterized by anomalous bathymetry and numerous hot spots. It has been suggested that the MPM record Pacific plate motion over such a superswell hot spot fixed in the deep mantle (*26*). This hypothesis is supported by our paleomagnetic data, because two guyots of the MPM (sites 865 and 866) appear to have formed at the same latitude (Fig. 5). Starting with site 866, we can calculate a synthetic APWP that would be created if the MPM record Pacific plate motion over a fixed hot spot (Fig. 4). We interpret the 95-million-year-old volcanic rocks recovered at site 171 to be indicative of the age of the eastern part of the potential hot spot track. When the synthetic APWP is compared with available paleomagnetic poles, the trend of the MPM suggests that longitudi-

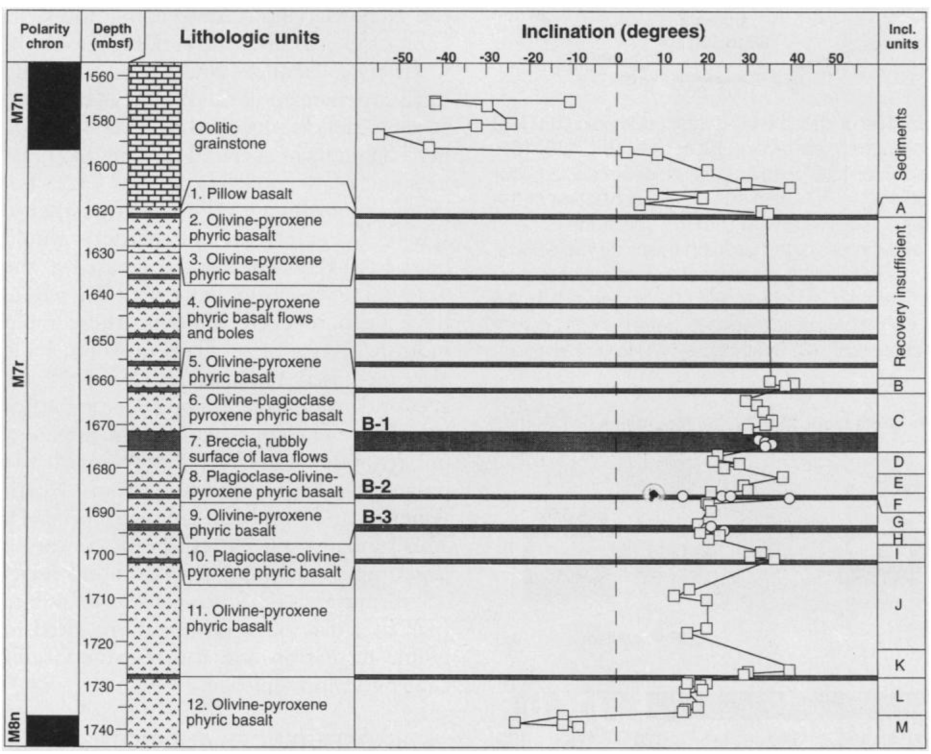

Fig. 2. Magnetic polarity chron (*17*), depth [meters below seafloor (mbsf)], lithology (*7*), characteristic inclinations, and inclination units (*16*) for site 866. Shaded levels represent weathered horizons (boles). B-1, B-2, and B-3 denote boles sampled for paleomagnetic analysis. Squares represent inclination values from basalts; circles are derived from bole samples. Note change in depth scale at 1620 mbsf.

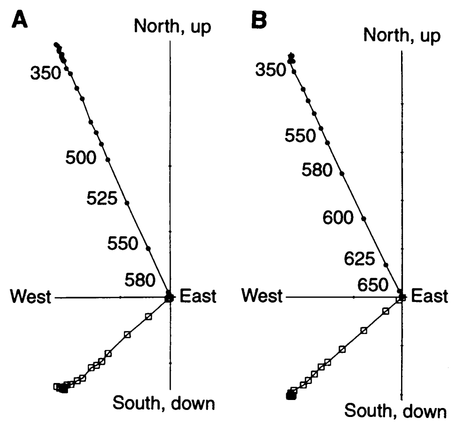

Fig. 3. Orthogonal vector plots of thermal demagnetizations (in degrees centigrade) of samples from site 866. (**A**) Basalt. (**B**) Bole sample. Open symbols are inclinations; solid symbols are declinations.

nal motion of the Pacific plate was also small from 128 to 90 Ma. For comparison, the total plate velocity suggested (~0.3° per million years) is only 16% of the velocity calculated for the Late Cretaceous (82 to 72 Ma) Pacific plate (*21*).

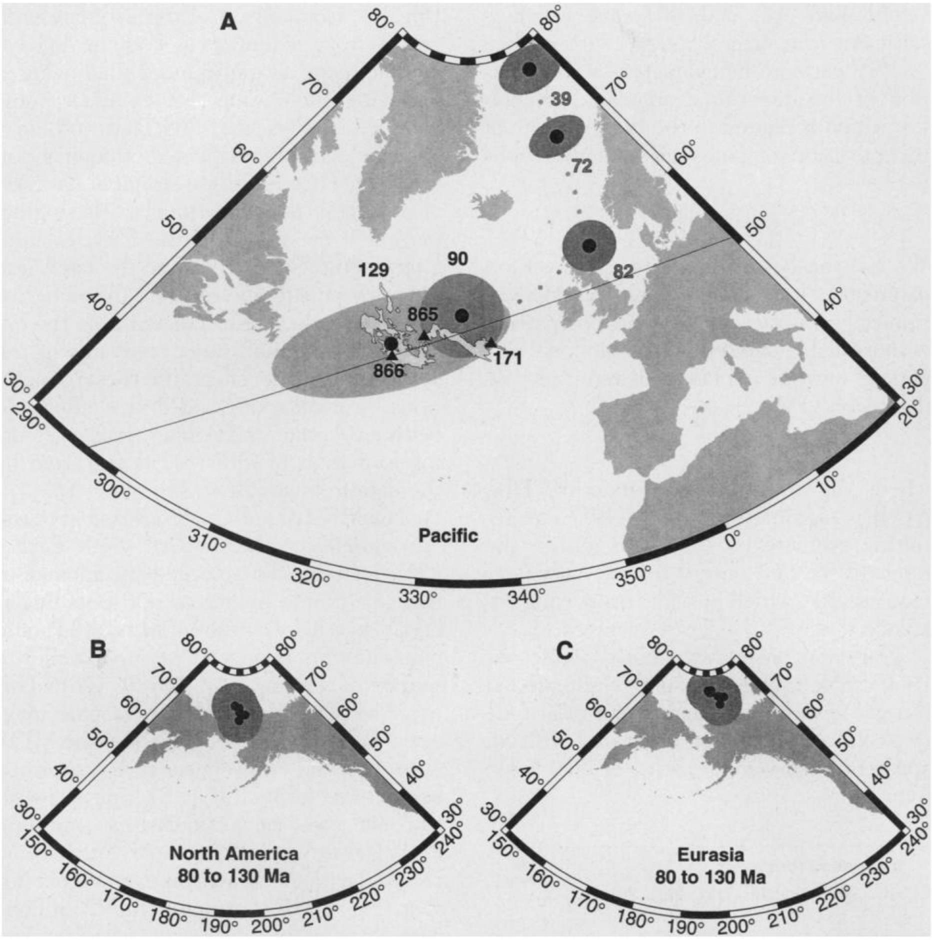

Fig. 4. (**A**) Pacific APWP (*21*) and MPM site 866 colatitude. The updated Early Cretaceous pole (129 Ma) (50.5°N, 323.3°E) is based on analysis (*14*) of basalt paleomagnetic data from DSDP sites 164, 166, 167, 289, 303, 304, and 462. The error ellipse has a major semiaxis of 13.9° with an azimuth of 64° and a minor semi-axis of 3.9°, $\chi^2 = 8.6$ with 5 degrees of freedom and $\chi^2_\nu = 1.7$. Also shown is a projection of the MPM, assuming they record a hot spot track. The synthetic path lies on the site 866 colatitude circle in the Early Cretaceous. The total polar motion cannot exceed the projected position of site 171 at 95 Ma. Although the synthetic path may lie anywhere along the site 866 colatitude circle, the total polar motion implied is within the error bounds of the Early to mid-Cretaceous (129 to 90 Ma) Pacific poles. (**B**) Synthetic APWP for Cretaceous North America based on global paleomagnetic data transfered to a common reference frame with the use of relative plate motions (*36*). (**C**) Synthetic APWP for Eurasia (*36*).

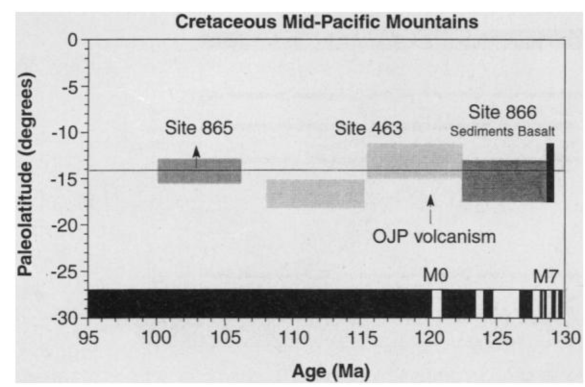

Fig. 5. Paleolatitude plot for the MPM. Data sets are assigned ages (*10*) on the basis of magnetostratigraphy and biostratigraphy. New radiometric age dates, which have not been incorporated into existing timescales, are not employed. Shown are site 865 data (shallow water limestones) (*23*), site 463 data (pelagic limestones) (*24*), site 866 sediments (shallow water sediments) (*17*), and site 866 basalts (presented here). The basalt mean (horizontal line) matches paleolatitude values from basalts and sediments of site 865 that are consistent with the MPM marking a hot spot track. When corrected for the difference in present-day site latitude (arrow above site 865 data), only minor latitudinal motion is suggested for the 128 to 100 Ma Pacific plate, which is inconsistent with plate motion changes initiating OJP volcanism.

Larson (*2*) considered the MPM (Cretaceous superswell) (*25*) to be the first manifestation of superplume activity. Because resistance to asthenospheric flow is lowest along a ridge axis where the low-viscosity channel height (h) is greatest and viscosity (μ) is least (*27*), the arrival of a large mantle plume head should affect rates of spreading. However, Pacific spreading rates as recorded by the Hawaiian lineations and calibrated by sedimentary sections in the Italian Southern Alps (*28*) are constant from chron M10 to chron M0 during the time of formation of the western MPM. In addition, isotopic anomalies linked to the superswell hot spots are >160 million years old (*29*), far older than the MPM or the Cretaceous volcanic episode. The MPM may have formed simply because the Pacific plate was nearly stationary for >30 million years above a preexisting hot spot (*30*).

Formation of the giant OJP, however, was sudden (*3*), ending a long period of constant spreading. We find no evidence for a change in plate motions that could have caused this event. Instead, we propose that the subsequent plate tectonic development of the mid-Cretaceous Pacific basin was a response to the mantle plume volcanism. While active, asthenospheric flow from the nascent OJP plume may have pinned the location of spreading ridges bounding the Pacific plate, as proposed for the present Southeast Indian Ridge, which may be fixed by asthenospheric flow from the Kerguelen and Amsterdam hot spots (*27*). Oceanic plates surrounding the Pacific (Izanagi, Farallon, and Phoenix) would have experienced ultrafast velocities (15 to 30 cm/year), as suggested in paleomagnetic investigations of accreted terranes (*31*) and in some plate modeling studies (*32*). Because replenishment of the Pacific asthenosphere by mantle plume activity would have both reduced μ and increased h, the drag force resisting plate motion would have been reduced, allowing these rapid motions. Rates of subduction would have also increased (*33*), as indicated by the ages and volumes of circum-Pacific batholiths (*34*). The episode of Pacific apparent polar wander standstill coincides with the polar standstill observed from North America (*35*) and Eurasia (*36*) (Fig. 4). This fundamental pattern points toward a lessening of mantle convection and related warming at the core-mantle boundary (*37*) that may have ultimately resulted in plume formation and the massive Cretaceous volcanic episode.

REFERENCES AND NOTES

1. S. O. Schlanger, H. C. Jenkyns, I. Premoli Silva, *Earth Planet. Sci. Lett.* **52**, 435 (1981).
2. R. L. Larson, *Geology* **19**, 547 (1991).
3. J. A. Tarduno *et al.*, *Science* **254**, 399 (1991).

4. J. J. Mahoney, M. Storey, R. A. Duncan, K. J. Spencer, M. Pringle, in *The Mesozoic Pacific: Geology, Tectonics, and Volcanism*, M. Pringle, W. Sager, W. Sliter, S. Stein, Eds. (Monograph 77, American Geophysical Union, Washington, DC, 1993), pp. 233–261.
5. M. A. Richards, R. A. Duncan, V. E. Courtillot, *Science* **246**, 103 (1989); M. A. Richards, D. L. Jones, R. A. Duncan, D. J. DePaolo, *ibid.* **254**, 263 (1991); M. F. Coffin and O. Eldholm, *Geology* **21**, 515 (1993).
6. D. L. Anderson, *Geology* **22**, 39 (1994).
7. W. W. Sager *et al.*, *Initial Report of the Ocean Drilling Program* **143** (ODP, College Station, TX, 1993).
8. H. C. Jenkyns, *Proc. Ocean Drill. Prog. Sci. Results*, **143**, 99 (1995).
9. A. Arnaud-Vanneau and W. V. Sliter, *ibid.*, p. 537.
10. F. M. Gradstein *et al.*, *Geophys. Res.* **99**, 24051 (1994).
11. M. Pringle and R. Duncan, *Proc. Ocean Drill. Prog. Sci. Results* **143**, 277 (1995).
12. All samples were azimuthally unoriented. Samples were thermally demagnetized at a minimum of 16 steps to 650° to 680°C (shipboard alternating field demagnetizations were ineffective on some samples, indicating the presence of a high-coercivity phase). After the removal of one or more components at low (50° to 200°C) unblocking temperatures, most basalt samples displayed a simple univectorial decay.
13. D. V. Kent and J. Gee, *Science* **265**, 1561 (1994).
14. R. G. Gordon and A. Cox, *Geophys. J. R. Astron. Soc.* **63**, 619 (1980); A. Cox and R. G. Gordon, *Rev. Geophys.* **22**, 47 (1984).
15. P. L. McFadden and A. B. Reid, *Geophys. J. R. Astron. Soc.* **69**, 307 (1982).
16. M. Kono, *Init. Rep. Deep Sea Drill. Proj.* **55**, 737 (1980). Inclination groups are distinct (at the 95% confidence level) if $Z > 1.96$, where

$$Z = (\bar{I}_1 - \bar{I}_2)/\sqrt{\frac{\sigma_1^2}{n_1} - \frac{\sigma_2^2}{n_2}},$$

$\bar{I}_1$ and $\bar{I}_2$ are the means of two adjacent inclination groups, σ_1 and σ_2 are their standard deviations, and n_1 and n_2 are the number of samples used in each inclination group. Site 866 inclination units were divided as follows: A-B, B-C, and C-D by intervening boles; D-E by lithology; E-F by inclination; F-G and G-H by intervening boles; H-I by inclination; I-J by intervening bole; J-K by inclination; K-L by intervening bole; and L-M by magnetic polarity.
17. J. A. Tarduno, W. W. Sager, Y. Nogi, *Proc. Ocean Drill. Prog. Sci. Results* **143**, 395 (1995).
18. R. T. Merrill and M. W. McElhinny, *The Earth's Magnetic Field: Its History, Origin and Planetary Perspective* (Academic Press, San Diego, CA, 1983).
19. A. V. Cox, *Geophys. J. R. Astron. Soc.* **20**, 253 (1970).
20. P. L. McFadden, R. T. Merrill, M. W. McElhinny, S. Lee, *J. Geophys. Res.* **96**, 3923 (1991).
21. R. G. Gordon, *ibid.* **95**, 8397 (1990); W. W. Sager and M. S. Pringle, *ibid.* **93**, 11753 (1988); R. L. Larson and W. W. Sager, *Proc. Ocean Drill. Prog. Sci. Results* **129**, 471 (1992).
22. W. W. Sun and K. P. Kodama, *J. Geophys. Res.* **97**, 19599 (1992); P. Arason and S. Levi, *ibid.* **95**, 4501 (1990); R. L. Larson, M. B. Steiner, E. Erba, Y. Lancelot, *Proc. Ocean Drill. Prog. Sci. Results* **129**, 615 (1992).
23. W. W. Sager and J. A. Tarduno, *Proc. Ocean Drill. Prog. Sci. Results* **143**, 399 (1995).
24. J. A. Tarduno, *Geophys. Res. Lett.* **17**, 101 (1990). Because of their latitude dependence, compaction-induced errors can be detected by an internal comparison of sediment data representing a wide range of site latitudes. Through such comparisons, only three sites (sites 463, 865, and 866) may have yielded data unaffected by compaction. Sediments from site 463 may have escaped the effects of compaction because of early silicification. Results from sites 865 and 866 are derived from shallow water carbonate rocks, which preserve detailed sedimentary structures showing little compaction.
25. M. K. McNutt and A. V. Judge, *Science* **248**, 969 (1990); M. K. McNutt, E. L. Winterer, W. W. Sager, G. Ito, *Geophys. Res. Lett.* **17**, 1101 (1990).
26. E. L. Winterer and C. V. Metzler, *J. Geophys. Res.* **89**, 9969 (1984); R. A. Duncan and D. A. Clague, in *The Ocean Basin and Margins*, vol. 7, *The Pacific Ocean*, A. Nairn, F. G. Stehli, S. Uyeda, Eds. (Plenum, New York, 1985), pp. 89–121; E. L. Winterer *et al.*, in *The Mesozoic Pacific: Geology, Tectonics, and Volcanism*, M. Pringle, W. Sager, W. Sliter, S. Stein, Eds. (Monograph 77, American Geophysical Union, Washington, DC, 1993), pp. 307–334.
27. J. Phipps-Morgan and W. H. J. Smith, *Nature* **359**, 524 (1992).
28. J. E. T. Channell and E. Erba, *Earth Planet. Sci. Lett.* **108**, 161 (1992).
29. R. R. Castillo, P. A. Floyd, C. France-Lanord, *Proc. Ocean Drill. Prog. Sci. Results* **129**, 405 (1992).
30. W. H. F. Smith, H. Staudigel, A. B. Watts, M. S. Pringle, *J. Geophys. Res.* **94**, 10501 (1989).
31. W. Alvarez, D. V. Kent, I. Premoli Silva, R. A. Schweikert, R. A. Larson, *Geol. Soc. Am. Bull.* **91**, 476 (1980); J. A. Tarduno, M. McWilliams, N. Sleep, *J. Geophys. Res.* **95**, 15503 (1990); J. A. Tarduno and M. Myers, *ibid.* **99**, 21691 (1994).
32. D. C. Engebretson, A. Cox, R. G. Gordon, *Geol. Soc. Am. Spec. Pap.* **206** (1985).
33. H. Staudigel and S. D. King, *Earth Planet. Sci. Lett.* **109**, 517 (1992).
34. R. L. Larson and W. C. Pitman III, *Geol. Soc. Am. Bull.* **83**, 3645 (1972).
35. B. R. Globerman and E. Irving, *J. Geophys. Res.* **93**, 11721 (1988).
36. J. Besse and V. Courtillot, *ibid.* **96**, 4029 (1991).
37. G. M. Jones, *ibid.* **82**, 1703 (1977).
38. We thank the University of Rochester for support from the Rochester Paleomagnetic Laboratory and L. Tauxe for use of the SIO Paleomagnetics Laboratory. GMT software from P. Wessel and W. H. F. Smith was used to make figures in this paper, and software from R. Gordon was used to calculate the 129-Ma pole. Supported by NSF.

2 March 1995; accepted 23 May 1995

Protein Reaction Kinetics in a Room-Temperature Glass

Stephen J. Hagen, James Hofrichter, William A. Eaton

Protein reaction kinetics in aqueous solution at room temperature are often simplified by the thermal averaging of conformational substates. These substates exhibit widely varying reaction rates that are usually exposed by trapping in a glass at low temperature. Here, it is shown that the solvent viscosity, rather than the low temperature, is primarily responsible for the trapping. This was demonstrated by placement of myoglobin in a glass at room temperature and subsequent observation of inhomogeneous reaction kinetics. The high solvent viscosity slowed the rate of crossing the energy barriers that separated the substates and also suppressed any change in the average protein conformation after ligand dissociation.

A physical understanding of protein structure and function is becoming increasingly important to biology (*1*). Since the pioneering work of Austin and others (*2*), myoglobin (Mb) has been the paradigm for such studies. At temperatures below the glass transition of the solvent ($T_g \approx 180$ K for 3:1 glycerol-water mixtures), the geminate ligand rebinding kinetics of Mb after photodissociation of its carbon monoxide complex are widely distributed, extending from microseconds to kiloseconds. These kinetics have been explained by the simple idea that Mb molecules at low temperature are "frozen" into conformational substates, each binding with a different exponential rate (*2*). At room temperature in water, geminate rebinding is nearly exponential (*3*), which indicates that the energy barriers that separate substates are sufficiently low for thermal averaging to occur on the nanosecond time scale at which rebinding occurs. From a study of the viscosity dependence of the conformational relaxation after ligand dissociation in Mb, Ansari *et al.* (*4*) suggested that the trapping of conformational substates at low temperature may result more from high solvent viscosity than from energy barriers internal to the protein. Here, we confirm this hypothesis by showing that Mb embedded in a glass at room temperature exhibits ligand binding kinetics similar to those observed at low temperature. The ligand binding rates are distributed, and there is no evidence for conformational relaxation after ligand dissociation. The averaged geminate rebinding rates in the glass are much higher than those of the relaxed protein, which points to the functional consequence of conformational relaxation. These studies suggest a reinterpretation of previous low-temperature kinetic data as well as a clarification of the relation between kinetics, neutron-scattering experiments (*5*), and molecular dynamics simulations of "glass-like" transitions in proteins (*6*).

Conformational changes play an important role in the kinetics of Mb as well as of hemoglobin. In aqueous solution at room temperature, the geminate rebinding of carbon monoxide to Mb is much slower than predicted by an extrapolation of the low-temperature distribution of geminate rates (*3*). In addition, the average rate of geminate rebinding decreases as the temperature is increased through the solvent-glass transi-

Laboratory of Chemical Physics, Building 5, National Institutes of Health, Bethesda, MD 20892–0520, USA.